

Indicial Lift Approximations for Two-Dimensional Subsonic Flow as Obtained from Oscillatory Measurements

J. G. Leishman*

University of Maryland at College Park, College Park, Maryland 20742

An approach is described to obtain generalized approximations to the indicial lift response due to angle of attack and pitch rate in two-dimensional subsonic flow. Starting from an assumed representation, the approximations are accomplished by means of a nongradient optimization algorithm in which the coefficients of the approximation are free parameters. The optimization is subject to prescribed constraints in terms of the known initial and asymptotic behavior of the indicial response, and by requiring the response duplicate the known exact (analytic) solutions at earlier values of time. The approach is applied to extract the intermediate forms of the indicial lift response, generalized in terms of Mach number and pitch axis location, from experimental measurements of the unsteady lift in the frequency domain.

Nomenclature

A_n	= coefficients of circulatory indicial functions
a	= sonic velocity, m/s
b_n	= poles of circulatory indicial functions
C_{α}, C_q	= lift transfer functions
C_n	= normal force coefficient
$C_{n\alpha}$	= normal force coefficient due to angle of attack
$\dot{C}_{n\alpha}$	= normal force (lift) curve slope in steady flow
C_{nq}	= normal force coefficient due to pitch rate
c	= airfoil chord, m
F, G	= real and imaginary parts of experimental lift response, respectively
$J, \bar{J}, \bar{\bar{J}}$	= objective functions
k	= reduced frequency, $\omega c/2V$
M	= Mach number
P	= penalty function
p	= Laplace variable
q	= normalized pitch rate, $\dot{\alpha}c/V$
S	= distance traveled by airfoil in semichords, $2Vt/c$
T_{α}, T'_{α}	= noncirculatory time constant due to α , in t domain and S domain, respectively
T_i	= universal noncirculatory time constant, c/a
T_q, T'_q	= noncirculatory time constant due to q , in t domain and S domain, respectively
t	= time, s
V	= freestream (or local) velocity, m/s
w	= weighting factors
x	= parameter vector
\bar{x}_a	= nondimensional pitch axis location aft of leading edge
z	= aerodynamic state vector
α	= angle of attack, rad
α_{eq}	= equivalent angle of attack during plunging, rad
β	= compressibility factor, $\sqrt{1-M^2}$
Γ	= vortex circulation strength, m^2/s
ϕ	= indicial response function
ω	= circular frequency, rad/s

Introduction

THE aeroelastic analysis of both fixed-wing and rotary wing aircraft relies on an accurate representation of the unsteady aerodynamics. Since the analyst is faced with the

problem of coupling the unsteady aerodynamic representation into the structural response model, this representation also must be in a convenient computational form. For fixed wing aeroelasticity, the analysis can often be carried out in the frequency domain, and well-established methods exist. However, many modern problems in aeroelasticity involve structural nonlinearities or feedback control systems that require the use of time-domain simulations. In rotary-wing aeroelasticity, it is especially important to formulate time-domain representations of the unsteady aerodynamics.

One versatile way to represent the unsteady aerodynamic loads on a typical section in response to an arbitrary forcing is through the use of indicial (step) response functions. The indicial response method is a fundamental approach to the problem, and affords considerable insight into the physical aspects of unsteady airfoil flows. One main advantage of the approach is that when the indicial response to a particular forcing mode is known, e.g., that due to angle of attack or pitch rate, the cumulative response to an arbitrary forcing can be obtained in the time-domain by means of Duhamel superposition. Such procedures are usually conducted numerically. Unsteady lift models using incompressible forms of the indicial response have been widely employed, e.g., Refs. 1-3. Unsteady lift models based on subsonic compressible flow forms of the indicial response are also in regular use and are given in discrete time form in Ref. 4 and in state-variable (ordinary differential equation) form in Ref. 5.

For incompressible flow, the indicial lift response was first derived by Wagner⁶ and is known exactly in terms of Bessel functions, see e.g., Von Karman and Sears,⁷ and Sears.⁸ In the majority of applications however, repetitive evaluations of Bessel functions (in the form of calls to a subroutine library) are impractical, and the Wagner function is usually approximated using sum of exponential functions. Another main advantage of using exponential functions to approximate the indicial response is that there exists a simple Laplace transform, and by that facilitates the use of various numerical schemes for arbitrary forcing. A common approximation to the Wagner function is the widely used Jones' exponential approximation⁹ with four coefficients (two poles). Recently, Peterson and Crawly,¹⁰ as well as Eversman and Tewari,¹¹ have obtained somewhat better exponential approximations to the Wagner function using an optimization process in which the approximation is extracted from the frequency domain result (Theodorsen solution). Yet, an exponential approximation can be made directly since the Wagner function is known exactly in terms of Bessel functions. In either case, improved exponential approximations to the Wagner function are more of academic interest and are only of limited practical

Received Jan. 14, 1992; revision received April 3, 1992; accepted for publication April 3, 1992. Copyright © 1991 by J. G. Leishman. Published by the American Institute of Aeronautics and Astronautics, Inc., with permission.

*Assistant Professor, Department of Aerospace Engineering, Member AIAA.

utility, since all real problems in aeroelasticity always involve compressibility effects to some degree.

In contrast to the incompressible case, the indicial responses in subsonic compressible flow are not exactly known. However, approximate results may be derived from the aerodynamic response due to harmonic motion. Mazelsky¹² made use of reciprocal relations between the theoretical lift on an oscillating airfoil in subsonic compressible flow and the indicial response. Approximate indicial response functions in exponential form are provided. In later work, Drischer¹³ applies the same approach to find exponential approximations for the indicial lift obtained during the penetration of a sharp-edge gust in subsonic flow. Another direct form of approach to find the indicial response from frequency domain data is discussed by Dowell.¹⁴ A limitation of all these approaches is that the aerodynamic response must be known over a wide range of reduced frequencies to accurately define the initial behavior of the indicial response. Although theoretical data usually exist over the required range, the range of experimental measurements is rather limited. This is mainly because of practical difficulties in obtaining high reduced frequencies at high subsonic Mach numbers, and so this poses some special problems in the extraction of the indicial response from experimental data.

The objective of this article is to describe an alternate derivation of generalized approximations to the indicial lift response for subsonic flow, mainly by using experimental data, but with the guidance of some exact solutions. Since it is impossible to obtain the indicial response directly from experiment, a derivation of the indicial function must be made by using results of the aerodynamic lift due to some other known forcing. This assumes that the aerodynamic system is linear, but this is normally the case for airfoils operating in nominally attached flow, even at high subsonic freestream Mach numbers. Based on the known behavior for the initial and asymptotic form of the indicial response, as well as known exact solutions for limited values of time, experimental measurements of the unsteady lift response in the frequency domain are used to help define the intermediate behavior the indicial response.

The procedure is applied in this article to the indicial lift responses due to angle of attack and pitch rate, however a similar approach can be used to find the corresponding indicial pitching moment responses, which are especially important for rotary wing applications. The main result of the present work are indicial lift functions, generalized in terms of Mach number and pitch axis location, that can be used in practical calculations to find the unsteady lift on an airfoil undergoing arbitrary motion or encountering an arbitrary gust field in subsonic flow.

Method of Analysis

Indicial Response

To illustrate the basic concept, assume that at some time the airfoil instantaneously attains a constant α and q about some axis. The perturbation velocity is therefore distributed across the chord in the form shown in Fig. 1. The resulting air loads are of a transient nature, and in subsonic flow only attain steady-state values after a significant amount of time. For a general pitching airfoil, two indicial functions are required. One corresponds to the uniform perturbation velocity due to angle of attack, and the other corresponds to a linear variation that is associated with the angular velocity about some pitch axis.

In contrast to the incompressible case, no analytic solutions are generally available for the indicial response in subsonic flow, except for very limited values of time. Even for the subsonic oscillatory case, the flow is governed by the Poisson integral equation for which there is no known exact analytical solution. There are also only a few published solutions for the indicial response using modern CFD approaches. There-

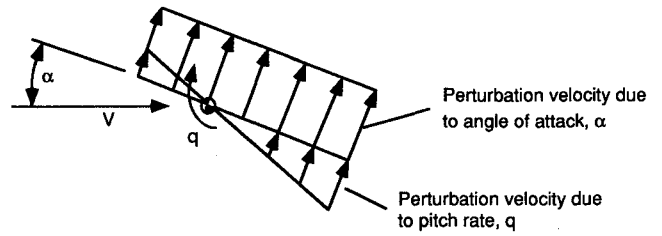


Fig. 1 Boundary conditions at airfoil surface in unsteady flow.

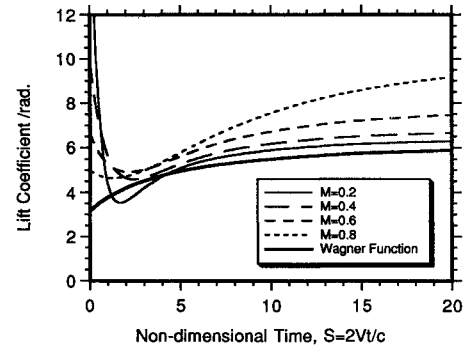


Fig. 2 Representative indicial lift responses due to a step change in angle of attack at various Mach numbers.

fore, the inclusion of compressibility effects makes the derivation of a convenient generalized representation of the indicial response a nontrivial task since there are few known solutions that can be used for reference.

Representative indicial lift responses to a step change in angle of attack are shown in Fig. 2 for three subsonic Mach numbers. Also shown for comparison in this figure is the more widely known Wagner function that is valid only for incompressible flow. The parameter $S (= 2Vt/c)$, by convention, represents the distance traveled by the airfoil in semichords. It is important to note that there is a considerable influence of Mach number on the indicial response functions. This manifests itself in two main ways. First, there is a finite- and time-dependent initial noncirculatory (or impulsive) behavior, compared to the incompressible case that exhibits an infinite pulse at time zero. Second, there is a more gradual asymptotic approach of the indicial lift to the final steady values compared to the incompressible case.

While the initial and final values of the indicial response are known exactly in subsonic flow, the intermediate behavior is only known exactly for very limited values of time. It has also been found that no simple compressibility scaling applies to the incompressible indicial result since the initial and final values, as well as the intermediate behavior, are all affected by compressibility in different ways. The indicial lift coefficients due to α and q (about some reference axis \bar{x}_a) can be approximated by the general equations

$$\Delta C_{n_\alpha}(S, M) = [(4/M)\phi_\alpha^i(S, M) + (2\pi/\beta)\phi_\alpha^c(S, M)]\Delta\alpha \quad (1)$$

$$\Delta C_{n_q}(S, M, \bar{x}_a) = \{[2(1 - 2\bar{x}_a)/M]\phi_q^i(S, M, \bar{x}_a) + (\pi/\beta)[(3 - 4\bar{x}_a)/2]\phi_q^c(S, M)\}\Delta q \quad (2)$$

where the indicial response functions $\phi_\alpha^c(S, M)$, $\phi_q^c(S, M)$, and $\phi_q^i(S, M, \bar{x}_a)$ represent the intermediate behavior of the indicial airloads between $S = 0$ and $S = \infty$. The optimal approximation and validation of these functions from experimental data constitutes the main objective of the present work.

Note that the total indicial response has been conveniently subdivided here into a sum of noncirculatory and circulatory parts; the superscripts c and i refer to the components of circulatory and noncirculatory (impulsive) loading, respectively. This idealized decomposition of the total loading into circulatory and noncirculatory parts is consistent with the work of Reissner¹⁵ and Mazelsky,¹⁶ and has been used more recently by Beddoes⁴ and Leishman.¹⁷ In the frequency domain this would be equivalent to breaking the solution into high and low frequency contributions, respectively. Since both the low and high frequency limit of the unsteady lift response in subsonic compressible flow is known exactly, this can be used to considerable advantage in the extraction of the indicial response.

Noncirculatory Lift

The noncirculatory loading comprises the initial air loading on the airfoil in response to a unit step change in the boundary conditions, as shown in Fig. 1. As discussed by Lomax,¹⁸ a direct physical interpretation of this air loading may be based on the energy of the acoustic wave system created by the initial perturbation. The initial air loading can be computed directly using piston theory where

$$\begin{aligned} \Delta C_{n\alpha}(S=0, M) &= (4/M)\Delta\alpha \quad \text{and} \quad \Delta C_{nq}(S=0, M, \bar{x}_a) \\ &= [2(1 - 2\bar{x}_a)/M]\Delta q \end{aligned} \quad (3)$$

These results are valid for any Mach number and for any pitch axis location, but only at the instant in time when the perturbation is applied.

Using reciprocal relations, Mazelsky¹⁶ successfully extracted the subsequent time-dependent behavior of the noncirculatory component from the total lift response computed for the harmonically oscillating case. Mazelsky showed that the noncirculatory lift in subsonic compressible flow decays rapidly from the initial (piston theory) values, but at a finite rate. This is due to the propagation of pressure disturbances at the speed of sound, compared to the incompressible case where disturbances propagate at infinite speed. The resulting noncirculatory lift decay exhibits some oscillatory overshoot of the zero lift asymptote, but can be closely approximated by an exponential function¹⁷ and may be written as

$$\begin{aligned} \Delta C_{n\alpha}^i(S, M) &= (4/M)\phi_{\alpha}^i(S, M)\Delta\alpha \\ &= (4/M)\exp\{-S/[T'_\alpha(M)]\}\Delta\alpha \end{aligned} \quad (4)$$

where $T'_\alpha(M)$ is a Mach number dependent decay rate or time constant. The noncirculatory indicial lift due to a step change in pitch rate can be approximated in a similar way. However, for this term it is necessary to take into account the pitch axis location so that we get

$$\begin{aligned} \Delta C_{nq}^i(S, M, \bar{x}_a) &= [2(1 - 2\bar{x}_a)/M]\phi_q^i(S, M, \bar{x}_a)\Delta q \\ &= [2(1 - 2\bar{x}_a)/M]\exp\{-S/[T'_q(M, \bar{x}_a)]\}\Delta q \end{aligned} \quad (5)$$

Circulatory Lift

The progressive buildup of the circulatory component of the indicial lift is due to the decreasing influence of the shed wake vorticity as it is convected away from the airfoil. The indicial lift response to a uniform change in the perturbation velocity or a step change in angle of attack ϕ_α^c has been shown to be proportional to the total lift obtained during the penetration of a sharp edge gust. This result was first given by Sears⁸ for the incompressible case, thereby connecting the Wagner step function to the Küssner gust function. Later, a similar result was given by Lomax¹⁹ for the subsonic com-

pressible flow case. The result was also generalized by Heaslet and Sprieter²⁰ by means of reciprocity relations.

As shown by numerous authors, including Drishler¹³ and Mazelsky,^{12,21} the circulatory part of the indicial response also can be adequately approximated by an exponential function and can be written in the general form

$$\begin{aligned} \Delta C_{n\alpha}^c(S, M) &= \frac{2\pi}{\beta} \phi_\alpha^c(S, M)\Delta\alpha \\ &= \frac{2\pi}{\beta} \left[1 - \sum_{i=1}^N A_i \exp(-b_i S) \right] \Delta\alpha \end{aligned} \quad (6)$$

where the A_i and b_i coefficients are all Mach number dependent. The steady-state values of the circulatory lift are simply the two-dimensional results given by the Prandtl-Glauert rule. Note that in practice, the linearized value of the steady lift-curve-slope, $2\pi/\beta$, in Eq. (6) should be replaced by value of the lift-curve-slope measured from experiment $\bar{C}_{n\alpha}(M)$.

While the form of the exponential approximation in Eq. (6) is acceptable for many applications in fixed wing aerelasticity (if the approximating coefficients at a given Mach number can be obtained by some means) it is still very inconvenient for a helicopter rotor analysis. This is because each blade station encounters a different local Mach number as a function of both blade station and azimuth angle. Thus, repeated interpolation of indicial coefficients between successive Mach numbers will be required in any application. Also, when superposition is applied, each exponential term in the series in Eq. (6) contributes an additional state in the aeroelastic analysis, and will quickly increase computational overheads. To economize on computational demands, a constraint is required to minimize the number of exponential terms, and ideally, to generalize these coefficients as a function of Mach number alone.

Beddoes⁴ proposed that the circulatory lift in subsonic compressible flow can be approximated by a two-term exponential function, the poles of which can be assumed to scale with β^2 , where β is the Prandtl-Glauert factor. The circulatory part of the total indicial response can be written as

$$\phi_\alpha^c(S, M) = 1 - A_1 \exp(-b_1 \beta^2 S) - A_2 \exp(-b_2 \beta^2 S) \quad (7)$$

Note, that for intermediate Mach numbers this scaling result is more representative and more accurate than simple linear interpolation of the b_n coefficients between successive Mach numbers for which the coefficients are known.

Beddoes selected the A_i and b_i coefficients in an indirect and nonoptimum manner, but based his result on a variety of detailed comparisons with both experimental and theoretical data sources, including finite-difference solutions and the indicial response results given in Bisplinghoff et al.⁹ It was clearly shown by Beddoes that for larger values of time, the poles of the indicial responses could be scaled in terms of the Mach number. However, as will be shown, Beddoes' values of the circulatory coefficients, namely $A_1 = 0.3$, $A_2 = 0.7$, $b_1 = 0.14$ and $b_2 = 0.53$, do not necessarily represent the optimum choice for a generalized indicial lift response function. Yet, we may assume that ϕ_α^c can still be written in the form

$$\phi_\alpha^c(S, M) = \phi_q^c(S, M) = 1 - \sum_{i=1}^N A_i \exp(-b_i \beta^\gamma S) \quad (8)$$

where the A_i and b_i terms, and the exponent γ are free parameters subject to the constraint that A_i , b_i , and γ are all greater than zero.

The form of the other circulatory function ϕ_q^c due to linear variation in perturbation velocity (pitch rate) must also be considered. Numerous references have shown that for incom-

pressible flow, the chordwise pressure variation on the airfoil due to the wake is the same as the thin airfoil loading, and is independent of the mode of motion. Therefore, an angular velocity about some point can be considered equivalent to an angular velocity about some other point plus an angle of attack. In particular, the indicial lift for a pitch rate about the $\frac{3}{4}$ -chord position in incompressible flow is impulsive at $S = 0$, and is exactly zero thereafter. Subsequently, it follows that for incompressible flow we may write $\phi_{\alpha}^c = \phi_q^c$.

In linearized subsonic flow, the circulatory lift lag still remains an intrinsic function of the fluid itself. The chordwise pressure variation due to the wake is still the same as the thin airfoil loading, and is unaffected by the mode of forcing or pitch axis location. Therefore, on a thin airfoil in subsonic flow, the lift always acts at the $\frac{3}{4}$ -chord point. This particular situation was examined in some detail by Mazelsky,²² who used exact numerical results for the unsteady lift and moment response in the frequency domain to extract the separate indicial responses due to angle of attack and pitch rate by means of reciprocal relationships. It was shown that at a Mach number of 0.7 for a pitching velocity imposed about the $\frac{3}{4}$ -chord, a nonimpulsive and finite time-dependent lift exists at $S = 0$ but approaches zero in as few as four semichord lengths of airfoil travel. The majority of this lift is of noncirculatory origin, and it is shown further in Ref. 22 that only the part of the lift response for $S > 4$ may be considered to be associated with circulation. This component is negligible, which is consistent with the incompressible result. It can be shown that a similar result applies at all other subsonic Mach numbers. The result for pitching about the $\frac{3}{4}$ -chord at $M = 0.8$ is given in Lomax,¹⁸ and in Ref. 9 for pitching about the leading edge at various Mach numbers. Therefore, the form of the time dependent and asymptotic buildup of circulatory lift due to pitch rate is identical to the buildup of lift due to angle of attack at all subsonic Mach numbers.

In view of the foregoing, it immediately becomes clear that we may write

$$\phi_{\alpha}^c(S, M) = \phi_q^c(S, M, \bar{x}_a) \quad (9)$$

for subsonic compressible flow as well as incompressible flow without any loss of rigor. Thus, the significance of the $\frac{3}{4}$ -chord point (or aft neutral point) is still maintained in unsteady subsonic flow. If required, the circulatory part of the total indicial lift response for an airfoil pitching about any axis can be obtained from the following transformation:

$$\begin{aligned} (\phi^c)_{\bar{x}_a}(S, M) &= \phi_{\alpha}^c(S, M) + [(3 - 4\bar{x}_a)/4]\phi_q^c(S, M) \\ &= [(7 - 4\bar{x}_a)/4]\phi_{\alpha}^c(S, M) \end{aligned} \quad (10)$$

Alternatively, we may write for the pitch rate contribution alone

$$(\phi_q^c)_{\bar{x}_a}(S, M) = [(3 - 4\bar{x}_a)/4]\phi_q^c(S, M) \quad (11)$$

which is the identical result given by Lomax in Ref. 18, but generalized here to an arbitrary pitch axis.

Derivation of the Noncirculatory Time Constants

During the intermediate time between the initial noncirculatory dominated loading until the final circulatory dominated loading is obtained, the flow adjustments are very complex and involves the propagation and reflection of pressure disturbances. To enable proper scaling of the basic physical effects, the exact linearized solutions to the subsonic indicial responses given by Lomax¹⁸ can be used to define the behavior of the loading for the period immediately after the step input. Lomax¹⁸ has obtained theoretical results for both the indicial lift and pitching moment due to a step change in angle of

attack, a step change in pitch rate, and for the penetration of a sharp edge gust. The mathematical calculations are somewhat complex, and solutions can be obtained only for a short period of time after the start of the motion (less than half a chord length of airfoil travel), but this is still sufficient to define the initial behavior of the indicial response. Lomax uses a more approximate analysis for larger values of time.

If the noncirculatory lift is assumed to decay with time in an exponential manner, as assumed previously in Eqs. (4) and (5), then the time constant for the noncirculatory lift decay can be approximated by equating the sum of the time derivatives of the assumed forms of the noncirculatory and circulatory lift response at time zero ($S = 0$) to the time derivative of the exact solutions obtained by Lomax. Based on this approach, which is outlined in Ref. 17, the noncirculatory time constants can be expressed in terms of the coefficients of the approximating circulatory function as

$$\begin{aligned} T_{\alpha}(M) &= \kappa_{\alpha} \left(\frac{c}{2V} \right) T'_{\alpha} = \kappa_{\alpha} \left[(1 - M) \right. \\ &\quad \left. + \pi\beta\gamma^{-1}M^2 \sum_{i=1}^N A_i b_i \right]^{-1} \left(\frac{c}{a} \right) = K_{\alpha}(M) T_i \end{aligned} \quad (12)$$

In a similar way, we can obtain the noncirculatory time constant associated with the linear perturbation velocity or pitch rate term. However, it is once again necessary to allow for the pitch axis location \bar{x}_a . After some manipulation it can be shown that, in general

$$\begin{aligned} T_q(M, \bar{x}_a) &= 2\kappa_q(1 - 2\bar{x}_a) \left[(1 - M)(1 - 2\bar{x}_a) \right. \\ &\quad \left. + 2\pi\beta\gamma^{-1}M^2 \sum_{i=1}^N A_i b_i \right]^{-1} \left(\frac{c}{a} \right) = K_q(M, \bar{x}_a) T_i \end{aligned} \quad (13)$$

This latter time constant applies for any pitch axis located a nondimensional distance \bar{x}_a aft of the airfoil leading edge. The constants κ_{α} and κ_q are assumed here to be free parameters in the ranges $0.70 \leq \kappa_{\alpha} \leq 1.0$ and $0.70 \leq \kappa_q \leq 1.0$. These constants somewhat modify the initial behavior of the indicial lift decay, and are justified because of additional physical effects such as airfoil thickness and minor viscous effects.

Note that in the above representation, the actual values for the circulatory coefficients A_i and b_i are nonessential since the noncirculatory time constants T_{α} and T_q will always be automatically adjusted to give the correct initial behavior of the total indicial lift response given by Lomax's exact linear theory. Also, it should be noted that the universal time constant T_i is the ratio of airfoil chord to the sonic velocity. Thus, as $a \rightarrow \infty$ (incompressible flow), $T_{\alpha} \rightarrow 0$ and the noncirculatory part of the lift becomes an infinite pulse at $S = 0$, which is a result consistent with incompressible flow theory.

Transfer Function

It has been previously explained why it is impossible to directly validate the above indicial response functions with experiment. However, by using convolution, it is straightforward to compute the lift to any prescribed motion and then relate these results back to the experimental data. Most experimental data in unsteady aerodynamics exist for pitch oscillations about the airfoil $\frac{3}{4}$ -chord at various frequencies and freestream Mach numbers. Unfortunately, there are very few published data for oscillating airfoils in subsonic flow about other pitch axes, and therefore the $\frac{3}{4}$ -chord pitch axis location will be assumed in all future discussion in this article. However, the results for pitching about any other axis can be easily computed by a simple transformation.

By the application of Laplace transforms to Eqs. (4), (5), and (8), the lift transfer functions due to angle of attack and

pitch rate about the $\frac{1}{4}$ -chord may be obtained explicitly. These lift transfer functions are

$$C_\alpha(p) = \bar{C}_{n_\alpha}(M) \left[\sum_{i=1}^N \frac{A_i}{1 + D_i p} \right] + \frac{4}{M} \left[\frac{T_\alpha(M)p}{1 + T_\alpha(M)p} \right] \quad (14)$$

$$C_q(p) = \bar{C}_{n_\alpha}(M) \left[\sum_{i=1}^N \frac{A_i}{1 + D_i p} \right] + \frac{1}{M} \left[\frac{T_q(M)p}{1 + T_q(M)p} \right] \quad (15)$$

where $D_i = c/2Vb_i\beta^\gamma$.

For a pure first harmonic pitch oscillation about the airfoil $\frac{1}{4}$ -chord axis at k , the forcing function is

$$\alpha_{3/4}(t) = \sin \omega t + (\omega c/2V) \cos \omega t = \sin \omega t + k \cos \omega t \quad (16)$$

and taking the Laplace transform we get

$$\alpha_{3/4}(p) = [\omega/(\omega^2 + p^2)] + [kp/(\omega^2 + p^2)] \quad (17)$$

Note that many sources of experimental measurements of unsteady airfoil data contain higher harmonic forcing terms superimposed on the fundamental, and it may be necessary to consider these effects in the analysis. By taking inverse Laplace transforms of the product of the transfer function and the forcing, the contributions to the lift from the angle of attack can be written explicitly as

$$\begin{aligned} \Re C_{n_\alpha}(k, M) &= \bar{C}_{n_\alpha}(M) \left(\sum_{n=1}^N \frac{A_n b_n^2 \beta^{2\gamma}}{b_n^2 \beta^{2\gamma} + k^2} \right) \\ &+ \frac{4}{M} \left(\frac{4k_\alpha^2 M^2 k^2}{1 + 4k_\alpha^2 M^2 k^2} \right) \end{aligned} \quad (18)$$

$$\begin{aligned} \Im C_{n_\alpha}(k, M) &= -\bar{C}_{n_\alpha}(M) \left(\sum_{n=1}^N \frac{A_n b_n \beta^\gamma k}{b_n^2 \beta^{2\gamma} + k^2} \right) \\ &+ \frac{4}{M} \left(\frac{2k_\alpha M k}{1 + 4k_\alpha^2 M^2 k^2} \right) \end{aligned} \quad (19)$$

where \Re and \Im denote the real and imaginary parts of the lift response, respectively. The corresponding contributions from the pitch rate are

$$\begin{aligned} \Re C_{n_q}(k, M) &= \bar{C}_{n_\alpha}(M) \left(\sum_{n=1}^N \frac{A_n b_n \beta^\gamma k^2}{b_n^2 \beta^{2\gamma} + k^2} \right) \\ &- \frac{1}{M} \left(\frac{2k_q M k^2}{1 + 4k_q^2 M^2 k^2} \right) \end{aligned} \quad (20)$$

$$\begin{aligned} \Im C_{n_q}(k, M) &= \bar{C}_{n_\alpha}(M) \left(\sum_{n=1}^N \frac{A_n b_n^2 \beta^{2\gamma} k}{b_n^2 \beta^{2\gamma} + k^2} \right) \\ &+ \frac{1}{M} \left(\frac{4k_q^2 M^2 k^3}{1 + 4k_q^2 M^2 k^2} \right) \end{aligned} \quad (21)$$

It will be apparent that the pitch rate contributions to the unsteady lift are of a smaller magnitude than the angle-of-attack terms, and only become important at higher frequencies. However, the contribution of these terms to the phasing of the air loads is considerably more important, and cannot be neglected. The effects of pitch axis location are also small, but nonnegligible.

Optimal Selection of Indicial Coefficients

The objective is now to find the optimal approximation for the coefficients used to define the intermediate behavior of the indicial lift approximations. This is achieved with the aid of an optimization algorithm. A $(2N + 3)$ -dimensional vector

can be defined that consists of the coefficients and poles used in the indicial response function, and also includes the exponent γ and factors κ_α and κ_q , i.e.

$$\mathbf{x}^T = \{A_1 A_2 \cdots A_N b_1 b_2 \cdots b_N \gamma \kappa_\alpha \kappa_q\} \quad (22)$$

Note that the noncirculatory time constants T_α and T_q do not appear in this vector since they are expressed implicitly in terms of the circulatory coefficients A_n and b_n [see Eqs. (12) and (13)]. This insures that the correct initial behavior of the indicial response for small values of time is always obtained no matter what the values of the circulatory coefficients. Note again, that the values of the circulatory coefficients are not affected by the mode of forcing or the pitch axis location.

The vector in Eq. (22) must be chosen to minimize the difference between the explicit solution based on the assumed indicial response approximations given in Eqs. (18–21), and the experimental measurements of the unsteady lift in the frequency domain. If the real and imaginary parts of the experimental data [$F_m(M_i)$ and $G_m(M_i)$, respectively] are known at up to M values of reduced frequency, and at each of I values of Mach number, an objective function $J(\mathbf{x})$ can be defined as

$$\bar{J} = \sum_{i=1}^I w_i J(\mathbf{x}, M_i) \quad (23)$$

where

$$\begin{aligned} J(\mathbf{x}, M_i) &= \sum_{m=1}^M [F_m(M_i) - \Re C_n(\mathbf{x}, M_i, k_m)]^2 \\ &+ [G_m(M_i) - \Im C_n(\mathbf{x}, M_i, k_m)]^2 \end{aligned} \quad (24)$$

The minimum of \bar{J} in the parameter space \mathbf{x} will give the best approximation to the experimentally measured lift transfer function. The weighting terms w_i are normally set close to unity.

The objective function minimization algorithm is basically a nonlinear programming problem of minimizing $\bar{J}(\mathbf{x})$ in the parameter space \mathbf{x} subject to the constraints

$$A_i, b_i, \gamma > 0 \quad i = 1, 2, \dots, N \quad (25)$$

$$0.70 \leq \kappa_\alpha, \kappa_q \leq 1 \quad (26)$$

$$\sum_{i=1}^N A_i = 1 \quad (27)$$

The latter equality constraint may be replaced by the exterior penalty function

$$P(\mathbf{x}) = R \left(\sum_{i=1}^N A_i - 1 \right)^2 \quad (28)$$

where R is a penalty parameter. Thus, we obtain the pseudo-objective function

$$\bar{J} = \sum_{i=1}^I w_i J(\mathbf{x}, M_i) + P(\mathbf{x}) \quad (29)$$

There are a variety of algorithms that can be employed to minimize $\bar{J}(\mathbf{x})$, but the nature of this particular problem (which includes sparse data and experimental errors) suggests the use of a nongradient method such as a direct search method. A number of different direct search methods were used in the present work with considerable success and rapid convergence. All methods used were found to produce essentially equivalent results for \mathbf{x} .

Arbitrary Forcing Theory from the Indicial Response

When the optimum approximation to the indicial response function has been found, the unsteady aerodynamic response to arbitrary forcing can be obtained. Starting from the transfer

function in Eq. (14), the circulatory part of the lift response can be written in state-variable form as

$$\begin{bmatrix} \dot{z}_1 \\ \dot{z}_2 \\ \vdots \\ \dot{z}_N \end{bmatrix} = \left(\frac{2V}{c}\right) \beta^\gamma \begin{bmatrix} -b_1 & 0 & \cdots & 0 \\ 0 & -b_2 & \cdots & 0 \\ 0 & \cdot & \cdots & 0 \\ 0 & \cdot & \cdots & -b_N \end{bmatrix} \begin{bmatrix} z_1 \\ z_2 \\ \vdots \\ z_N \end{bmatrix} + \begin{bmatrix} 1 \\ 1 \\ \vdots \\ 1 \end{bmatrix} \alpha_{3/4}(t) \quad (30)$$

$$A = \begin{bmatrix} -(2V/c)\beta^\gamma b_1 & \cdot & \cdot & \cdot & 0 & 0 & 0 \\ 0 & -(2V/c)\beta^\gamma b_2 & \cdot & \cdot & \cdot & \cdot & 0 \\ 0 & \cdot & \cdot & \cdot & \cdot & \cdot & 0 \\ 0 & \cdot & \cdot & \cdot & -(2V/c)\beta^\gamma b_N & \cdot & 0 \\ 0 & 0 & 0 & \cdot & \cdot & -1/k_\alpha T_i & 0 \\ 0 & 0 & 0 & 0 & 0 & 0 & -1/k_q T_i \end{bmatrix} \quad (38)$$

where $\dot{z} = dz/dt$. The corresponding output equation for the circulatory lift coefficient is given by

$$C_n^c(t) = \bar{C}_{n\alpha} \left(\frac{2V}{c}\right) \beta^\gamma [A_1 b_1 \quad A_2 b_2 \quad \cdots \quad A_N b_N] \begin{bmatrix} z_1 \\ z_2 \\ \vdots \\ z_N \end{bmatrix} \quad (31)$$

Note the use of the angle of attack at $\frac{3}{4}$ -chord, i.e.

$$\alpha_{3/4}(t) = \alpha(t) + [q(t)/2] \quad (32)$$

which is in accordance with the thin airfoil result in both incompressible and compressible flow. The use of Eq. (32) also has the advantage that the number of circulatory state variables are reduced by a factor of two over the case when the pitch rate terms are retained explicitly. However, it will be recognized that this can only be justified for the circulatory parts, since the noncirculatory terms produce different forms of chordwise loading, and the subsequent decay (time-history) of these noncirculatory loadings are governed by different time constants that also depend on the pitch axis location.

The noncirculatory lift coefficient due to angle of attack can be written in state-variable form as

$$\dot{z}_{N+1} + (1/k_\alpha T_i) z_{N+1} = \alpha(t) \quad (33)$$

and the corresponding state-variable representation of the noncirculatory lift due to pitch rate as

$$\dot{z}_{N+2} + (1/k_q T_i) z_{N+2} = q(t) \quad (34)$$

The output equations for the components of the noncirculatory lift coefficient are given by

$$C_{n\alpha}^i(t) = (4/M) \dot{z}_{N+1} = (4/M) [\alpha(t) - (1/k_\alpha T_i) z_{N+1}] \quad (35)$$

$$C_{nq}^i(t) = (1/M) \dot{z}_{N+2} = (1/M) [q(t) - (1/k_q T_i) z_{N+2}] \quad (36)$$

Note that the last two terms are just the compressible analogs of the apparent mass terms used for incompressible flow. The main difference is that the compressible quantities depend on

the time history of the forcing, whereas the so-called apparent mass terms are proportional to the instantaneous forcing.

The state equations representing the unsteady aerodynamic response can be grouped in the matrix form

$$\begin{bmatrix} \dot{z}_1 \\ \dot{z}_2 \\ \vdots \\ \dot{z}_N \\ \dot{z}_{N+1} \\ \dot{z}_{N+2} \end{bmatrix} = [A] \begin{bmatrix} z_1 \\ z_2 \\ \vdots \\ z_N \\ z_{N+1} \\ z_{N+2} \end{bmatrix} + \begin{bmatrix} \alpha_{3/4}(t) \\ \alpha_{3/4}(t) \\ \vdots \\ \alpha_{3/4}(t) \\ \alpha(t) \\ q(t) \end{bmatrix} \quad (37)$$

where the aerodynamic state matrix is

$$A = \begin{bmatrix} 0 & 0 & 0 & 0 \\ \cdot & \cdot & \cdot & 0 \\ \cdot & \cdot & \cdot & 0 \\ \cdot & \cdot & \cdot & 0 \\ -(2V/c)\beta^\gamma b_N & \cdot & \cdot & 0 \\ \cdot & -1/k_\alpha T_i & \cdot & 0 \\ 0 & 0 & 0 & -1/k_q T_i \end{bmatrix} \quad (38)$$

These equations can be solved simultaneously at successive intervals of time for an arbitrary variation in α and q by using a standard ordinary differential equation solver. The individual components of aerodynamic loading are finally combined to obtain the overall aerodynamic response of the airfoil, i.e.

$$C_n(t) = C_n^c(t) + C_{n\alpha}^i(t) + C_{nq}^i(t) \quad (39)$$

Results and Discussion

Frequency Domain Results

Experimental data are available from a number of sources that comprise the unsteady aerodynamic lift response (or lift transfer function) due to pitch as well as plunge oscillations performed under nominally attached flow conditions, i.e., in the regime where linearized aerodynamics are appropriate. It is essential that the selected data be for attached flow conditions since the presence of even minor nonlinearities due to separation effects introduces further complications into the extraction of the indicial lift response.

Ideally, both pitch and plunge data are desirable, since the absence of contributing aerodynamic terms due to pitch rate in the plunge oscillations makes it possible, in principle, to isolate angle-of-attack contributions in the pitch oscillations. However, as recently shown in Ref. 23, measurements of the unsteady lift for plunge forcing are somewhat limited in terms of both reduced frequency range and Mach number, and also seem to exhibit more random experimental errors than is desirable. This latter effect is partially due to the difficulties in defining an "equivalent" angle of attack for plunge oscillations in terms of the plunge velocity and local freestream velocity. For these reasons, plunge oscillation data were not directly used in the present work. Pitch oscillation tests are considerably more numerous, with much less scatter between airfoils and test facilities. Therefore, these data provide a better basis for the meaningful extraction of the indicial lift response.

For this article, oscillatory pitch aerodynamic data were taken mainly from three sources: 1) the Boeing facility as documented by Liiva et al.²⁴; 2) the Aircraft Research Association (ARA) facility, as documented by Wood²⁵; and 3) the NASA transonic facility as documented by Davis and Malcolm.²⁶ All data are for pitching oscillations about the airfoil $\frac{3}{4}$ -chord. Other experimental measurements documenting the unsteady lift of oscillating airfoils certainly exist and have been used, but they are much more limited in terms

of reduced frequency range, Mach number range, or are at too low a Reynolds number to be useful for the present study. To put all the experimental measurements on a common basis, the lift amplitudes of the response were normalized with respect to the measured static lift curve slope. For presentation, the lift amplitude has been postmultiplied by the linearized value of $2\pi/\beta$ to clarify the effects of Mach number. The average experimental error in the experimental data was estimated to be ± 0.02 for the lift amplitude and ± 3 deg for the phase angle.

In each case, the optimal approximation to the indicial response coefficients A_i , b_i , γ , κ_1 , κ_2 was sought by minimizing the objective function in Eq. (29) for each experimental data set in turn. The results for the equivalent lift transfer function were then recompared against the experimental measurements in the frequency domain. Initial studies led to two observations. First, it was possible to obtain satisfactory results with a low objective function using as few as one circulatory lift term, i.e., $N = 1$. This is useful since as few circulatory terms as possible are necessary to minimize the number of states in the aeroelastic analysis, e.g., Eq. (37). However, solutions with $N = 2$ were notably better, with a much lower overall objective function. There was no significant decrease in the objective function when using more than two circulatory terms, and therefore, only two circulatory terms were retained in all subsequent studies. Second, the values of γ obtained from the optimizer were consistently close to 2, and usually ranged from 1.8 to about 2.3. Therefore, for consistency and simplicity in the remainder of this study, the value $\gamma = 2$ was used. This means that the poles of the circulatory part of the indicial response scale with $\beta^2 = (1 - M^2)$, which is in agreement with the earlier work of Beddoes.⁴ This result can also be deduced for later values of time from the indicial results published by Bisplinghoff.⁹ As will be shown, in the frequency domain this Mach number scaling of the indicial lift response is particularly evident at low reduced frequencies where the circulatory terms are much more dominant.

Boeing Data

Unsteady data from the Boeing 4×4 ft supersonic wind tunnel are for freestream Mach numbers of 0.2, 0.4, and 0.6, and for a fairly wide range of reduced frequencies. Data for two airfoils, namely the symmetric NACA 0012 and the cambered NACA 23010, are included. The Boeing data are quite unique since a few measurements were made at a very high reduced frequency of 0.72, albeit at the lowest Mach number. However, this provides a rare opportunity to examine the higher frequency end of the unsteady lift response where the noncirculatory loads are more dominant.

A comparison of the optimized transfer function with the Boeing data are shown in Fig. 3. It can be clearly seen that the effects of compressibility on the unsteady lift response are very significant. There is a fair correlation of the optimized lift transfer function with the lift amplitude at all three Mach numbers, and for both airfoil sections. The lift amplitude shows an initial attenuation with increasing frequency, followed by an increasing trend due to the buildup of the noncirculatory loads. Recall that this effect is qualitatively predicted by incompressible (Theodorsen's) theory.

The effects of compressibility on the phase angle of the lift response are particularly apparent in the lower part of Fig. 3, where there is an increasing phase lag with increasing Mach number in the low reduced frequency range. At the higher reduced frequencies, the noncirculatory parts of the lift response become more significant, and the change in the sign of the phase angle (from a lag to a lead) near a reduced frequency of 0.3 is due to the increasing contribution from the noncirculatory terms. For higher reduced frequencies, the noncirculatory loads dominate the overall response.

In general, the phase of the optimized lift response correlated fairly well with the test data, however, it can be seen

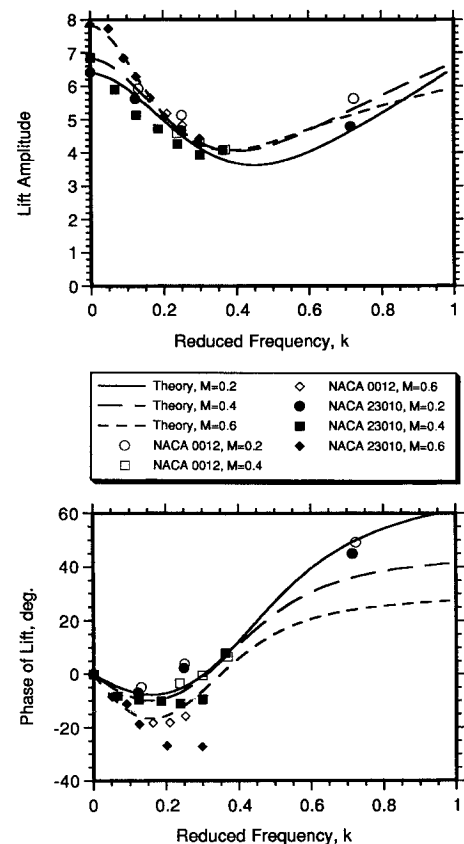


Fig. 3 Unsteady lift amplitude and phase angle for Boeing data.

from the lower part of Fig. 3 that there is somewhat more scatter of the phase angle between the NACA 0012 and NACA 23010 airfoils, especially at $M = 0.6$. As will be shown, the larger phase lag angles of the unsteady lift response for the NACA 23010 airfoil appears somewhat of an anomaly compared to other experimental measurements for cambered airfoils at the same (or higher) Mach numbers. The reason for this is not clear, but it is possibly a nonlinear effect related to the formation of some limited amounts of flow separation since these particular test points were for somewhat higher mean angles of attack.

ARA Data

Unsteady lift data from the ARA 18×8 -in. intermittent blowdown wind tunnel is for a NACA 0012 airfoil. The data covers a comprehensive range of Mach numbers from 0.3 to 0.75, but only up to reduced frequencies of 0.25. Nevertheless, relatively high reduced frequencies were obtained at higher Mach numbers of 0.7 and 0.75, and these data provide further scope for a better overall definition of the indicial response.

A comparison of the optimized lift transfer function with the first harmonic lift amplitude and phase of these test data are shown in Fig. 4. It can be seen that the lift amplitude correlated extremely well with the test data over the full range of Mach numbers. Despite the limited range of reduced frequencies of these test data, the smaller Mach number increment also resulted in a lower overall objective function. It can be seen in the lower part of Fig. 4, that the phase angle of the unsteady lift response increases dramatically in the low frequency range as the freestream Mach number exceeds 0.6. This large rate of change of phase angle with Mach number at a constant reduced frequency reiterates the necessity of including compressibility effects in any aeroelasticity analysis, even for low reduced frequencies and at Mach numbers as low as 0.6. This is typically below the Mach numbers where strong shock waves would be expected to appear on the NACA

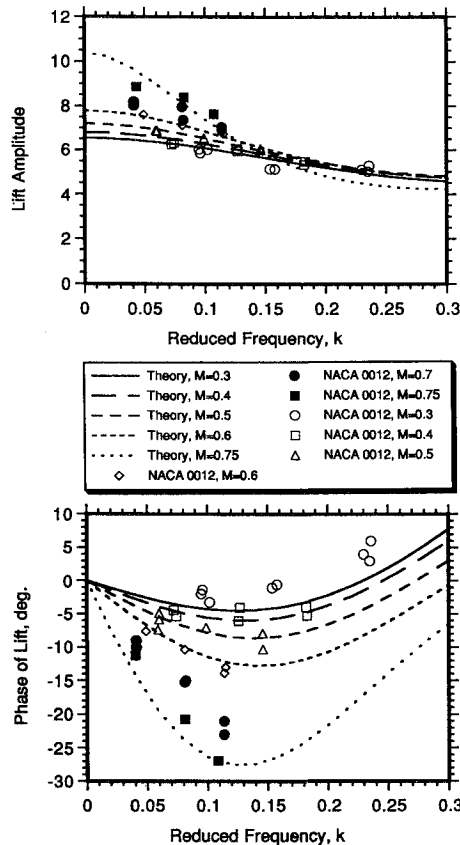


Fig. 4 Unsteady lift amplitude and phase angle for ARA data.

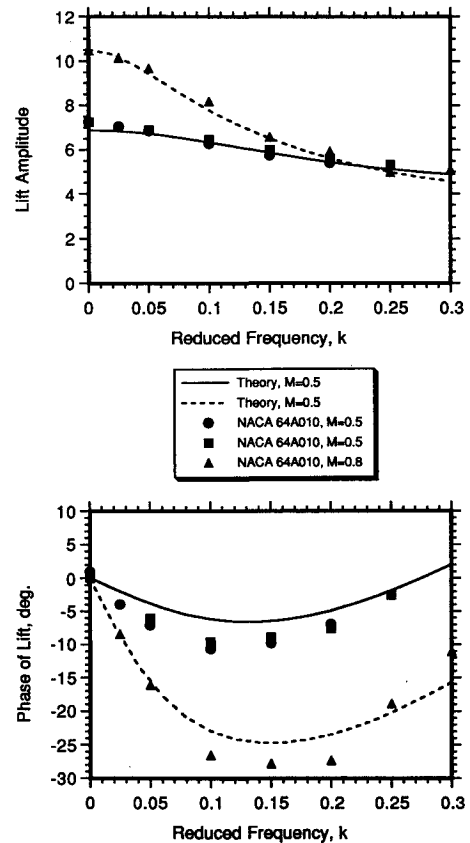


Fig. 5 Unsteady lift amplitude and phase angle for NASA data.

0012, and thus the large phase lag in the lift response is clearly not a nonlinear transonic effect, as is sometimes implied.

Note that the high frequency (piston theory) limit was still imposed in these calculations, and no attempt was made to relax this constraint to decrease the objective function for the somewhat limited frequency range of these data. While this can be done, it is not a fully satisfactory option since the predicted unsteady aerodynamic response in the time domain will be compromised for transient type changes in angle of attack or for higher frequency angle of attack variations.

NASA Data

The experimental measurements obtained by Davis and Malcolm²⁶ from the NASA facility are for a supercritical NACA 64A010 airfoil. Data were recorded for Mach numbers of 0.5 and 0.8, and for small angle-of-attack oscillations at reduced frequencies up to 0.3. Even with a somewhat high freestream Mach number of 0.8, the extent of transonic flow over the supercritical NACA 64A010 airfoil is quite limited, and nonlinear effects are negligible. Therefore, linear theory would be expected to prevail for these conditions, and these data provide for further definition of a generalized indicial response function.

A comparison of the optimized transfer function with the NACA 64A010 unsteady lift amplitude and phase angle is shown in Fig. 5. Again, the same general trends shown previously are observed for increasing frequency and increasing Mach number. The significant reduction in the unsteady lift amplitude with increasing reduced frequency for the higher Mach number of 0.8 is particularly noticeable in this case. This is mainly a circulatory effect, since the noncirculatory loads do not build up to affect the amplitude of the lift response to any extent until k exceeds about 0.25. Note that for a Mach number of 0.8, a maximum lift phase lag of about 30 deg for the NACA 64A010 airfoil compared with similar values obtained at a Mach number of 0.6 with the NACA 23010 airfoil, as shown previously in Fig. 3.

Consolidated Data

It is clear from the foregoing that there is a certain amount of scatter in the measurements of the unsteady lift, both between different airfoil sections, and even between the same airfoil (NACA 0012) tested in different wind-tunnel facilities. Some measurements appear anomalous, for example the NACA 23010 data set at $M = 0.6$. However, generally good agreement was obtained in the estimation of an optimum lift transfer function from the various data sets. It can be seen from Table 1 that the coefficients representing the corresponding indicial response functions strongly depend on the actual experimental data set used. This is because of the widely varying range of Mach numbers and reduced frequencies obtained in each of the test facilities. It is indeed unfortunate that there is no one set of published unsteady lift data that covers both a wide range of reduced frequencies, Mach numbers, and airfoils operating in fully attached flow. It is apparent that the lack of these data poses many practical problems in the extraction of the indicial response (by whatever method) from experimental measurements.

In view of the limited data from any one source, in the next part of the study the results from the various tests were consolidated into one data set for the optimization process and the extraction of a final indicial response function. The range of the experimental data used therefore covers Mach numbers from 0.2 up to 0.8, and is mainly for reduced frequencies up to 0.3. Note that the two data points for the NACA 0012 at $k = 0.72$ were retained. However, the apparently anomalous NACA 23010 data set at $M = 0.6$ was removed for this calculation.

A comparison of this (final) generalized transfer function with the unsteady lift amplitude and phase angle is shown in Fig. 6. Only selected experimental data are shown in this plot for clarity, but the final result can be easily compared with the other data shown in previous plots. It can be seen that the agreement of the theory with both the amplitude and phase is very good, both at the low and high frequency ends

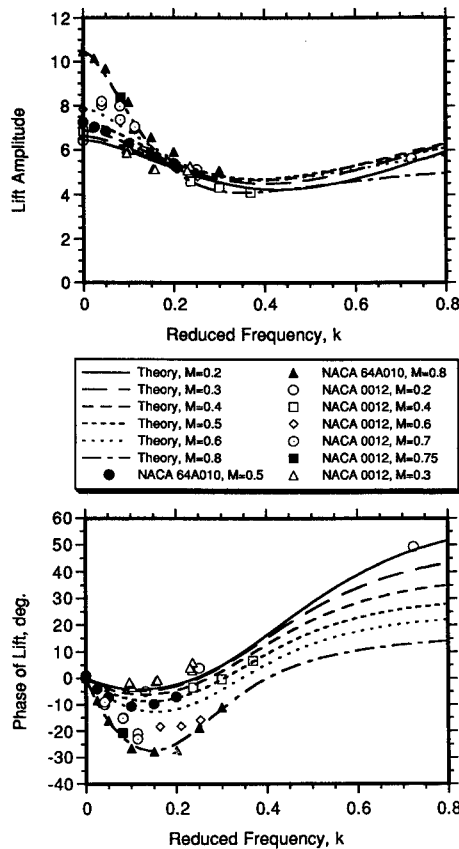


Fig. 6 Unsteady lift amplitude and phase angle for data for consolidated data set.

Table 1 Coefficients of derived indicial lift approximations

Data source	A_1	A_2	b_1	b_2	κ_1	κ_2
Boeing ²⁴	0.636	0.364	0.339	0.249	0.77	0.70
ARA ²⁵	0.625	0.375	0.310	0.312	1.00	1.00
NASA ²⁶	0.482	0.518	0.684	0.235	0.72	0.70
All data	0.918	0.082	0.366	0.102	0.85	0.73

of the spectrum. Overall, it is clear that the effects of Mach number on the phase angle are extremely strong, particularly at reduced frequencies below 0.3, and again in the higher frequency range. Note that the phase lead obtained at higher reduced frequencies is strongly affected by Mach number, whereas the effect on the lift amplitude is relatively small. The coefficients of the corresponding indicial lift function obtained from the consolidated experimental data set are given in Table 1.

Comparison with CFD Indicial Result

It is interesting to compare the derived approximation of the indicial lift response with a result from a modern finite-difference (CFD) method, even though these results are very limited in the published literature. The present results for both the total indicial lift response and the circulatory part alone are plotted in Fig. 7 for $M = 0.8$. These results are compared with the recent indicial calculations performed by McCroskey²⁷ using transonic small-disturbance theory. As noted previously, the circulatory part of the indicial response to a step change in angle of attack is identical with the total lift obtained during the penetration of a sharp-edge gust. The distance traveled by the airfoil (time) is plotted here on a logarithmic scale, and serves to significantly accentuate the nature of the response and the differences in the solutions at small values of time. It can be seen that the approximations

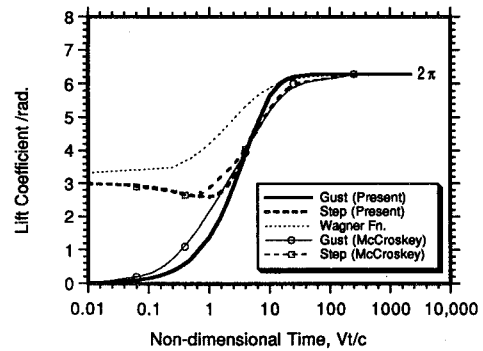


Fig. 7 Indicial lift response compared with TSD result at $M = 0.8$.

are in good agreement with the CFD results, and therefore, give significant credibility to both the CFD results themselves (which were not validated in Ref. 27), as well as the approximate indicial response functions derived in this article from experimental measurements.

Application of Arbitrary Forcing Theory

Unsteady Lift During Pitch and Plunge Oscillations

While the lift transfer functions are of considerable interest and value, further verification as to the validity of the indicial lift functions can be gained by comparing the results from the arbitrary forcing theory with the actual time-histories of the unsteady lift that comprised some of the test points previously considered. Consider an application to the prediction of the unsteady lift on the NACA 23010 airfoil undergoing harmonic pitch and plunge (heave) oscillations at $M = 0.4$. Experimental data were taken from the work of Liiva et al., and the test data were reconstructed from the harmonics published in Ref. 24. Note that these tests comprise the only source of published data where the airloads for both pitch and plunge oscillations were measured at significant subsonic Mach numbers, and offers a good opportunity to delineate the effects of the pitch rate contributions to the lift.

For these simulations, the integration of the state equations representing the unsteady aerodynamic behavior was performed using the ODE solver DE/STEP given in Ref. 28. This is a general purpose Adams-Bashforth solver with variable step size and variable order. Relative and absolute numerical tolerances of 10^{-12} were imposed on the solution. The measured static lift curve slope and zero lift angle for the NACA 23010 airfoil at $M = 0.4$ were used as inputs for these calculations.

Typical calculations for the normal force in attached flow are shown in Fig. 8 for harmonic pitch forcing (upper figure) and for harmonic plunge forcing (lower figure). The elliptical shaped normal force loops shown in Fig. 8 are typical for oscillatory forcing under unsteady attached flow conditions. In both the pitch and plunge cases, the unsteady lift lags the forcing at these relatively low reduced frequencies, and therefore, the hysteresis loops are traversed in a counterclockwise direction. Overall, the agreement of the theory with the experimental data is very good, and the predictions certainly fall within the bounds of experimental uncertainty.

Note that the pitch and plunge data shown in Fig. 8 are for approximately the same reduced frequency and mean angle of attack, and essentially serve to illustrate the effects of the pitch rate contributions to the unsteady lift. Although it is obvious that the equivalent angle of attack amplitude induced during plunge forcing is not exactly the same for pitching, this is not a serious factor in the attached flow regime since the results are linear functions of angle of attack. The plunge oscillation loops are slightly "fatter"—that is the phase lag angle for plunge is slightly greater than for pitching at (approximately) the same reduced frequency. This is because the pitch rate contributions to the unsteady lift in the pitching

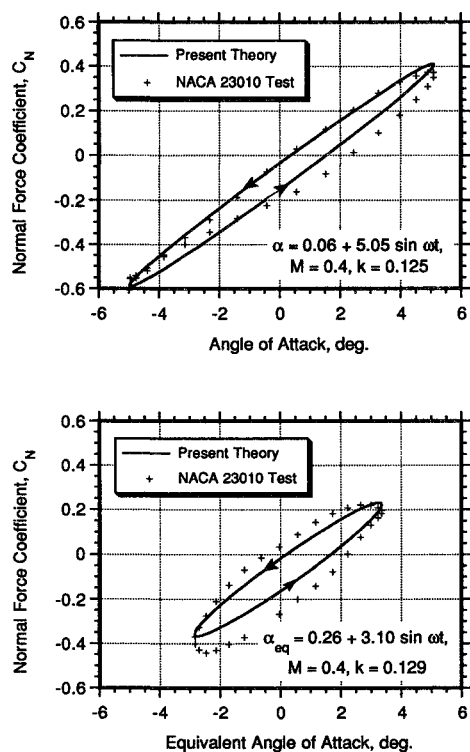


Fig. 8 Prediction of unsteady lift for pitching and plunging oscillations.

oscillation case causes a small phase lead. This is mainly a circulatory effect, since at this reduced frequency the noncirculatory contributions are small, though they are certainly not negligible.

Additional results were computed at other Mach numbers and reduced frequencies, with similar levels of agreement with the experimental data. This lends further confidence to the forms of the indicial lift response used here. A further discussion on the general effects of pitch versus plunge forcing on the unsteady lift and pitching moment (including dynamic stall) is given in Ref. 23.

Unsteady Lift and Noise During Blade Vortex Interaction

As an application that exercises the full range of the derived indicial response function, consider the application of the arbitrary forcing theory to a transient-type problem such as an airfoil-vortex interaction. On a helicopter rotor there are a large number of vortical disturbances that lie in proximity to the blades. This is especially the case for the advancing side of the rotor when the helicopter is descending, where the blades may repeatedly encounter a number of close and almost parallel interactions with wake vortices. This so-called blade vortex interaction (BVI) problem is a highly unsteady phenomenon, and is a significant source of higher harmonic airloads, as well as obtrusive noise that is known as "blade-slap." This makes the BVI problem of great practical significance.

The BVI problem was studied for incompressible flow by Sears²⁹ using the sharp-edge gust entry lift function (Küssner function) along with Duhamel superposition. For subsonic compressible flow, there have been many significant theoretical contributions to the BVI problem, e.g., Refs. 30 and 31 and the references contain therein. However, since transonic effects are often present, there has been considerably more progress in understanding this BVI problem in light of recent developments in CFD (e.g., Refs. 32 and 33 and the references contained therein). However, one major problem that remains is the satisfactory prediction of the unsteady lift (and noise) due to BVI by means of the somewhat simpler

aerodynamic models that are always necessary for use in comprehensive helicopter rotor analyses.

It is significant to note here that many currently used helicopter rotor analyses exhibit a nonphysical oversensitivity of the predicted airloads and noise due to BVI (e.g., example the work in Ref. 34). This is partly due to inadequate modeling of the inherent unsteady effects, but is particularly due to a lack of proper compressibility modeling. This problem is frequently disguised by attenuating the peak-to-peak lift response by the use of an artificially large vortex core radius, thereby attenuating the strength of the interaction. A solution such as this, of course, is rather unsatisfactory. Yet, it will become clear that this will approximately produce the desired effect on the peak-to-peak airloads, but not necessarily the temporal phasing of these loads.

An example of predictions that can be made using the present model for a BVI encounter are shown in Fig. 9. The convecting vortex is of strength $\hat{\Gamma} = \Gamma/cV = 0.2$ and has an irrotational core. The vortex travels at a steady velocity at 0.26 chords below a NACA 0012 airfoil. This is a standard case that has received considerable attention in the literature.³³ While passing the blade (airfoil) at this predetermined distance the vortex produces a downwash, while upstream of the airfoil that changes to an upwash as it moves downstream. This situation causes a dynamically changing angle of attack, and so rapidly changing aerodynamic loads are produced on the airfoil. On a helicopter rotor, the acoustic pressure (or noise) propagated to an observer from such a blade-vortex encounter is related (in the compact source limit) to the time rate of change of the aerodynamic lift. Thus, a prerequisite to rotor BVI noise prediction is an accurate model for the unsteady aerodynamics.

The angle-of-attack variation induced by the passing vortex was used in conjunction with the state equations in Eq. (31) to solve for the unsteady lift. This solution essentially parallels the classical problem of Duhamel superposition with the Küssner function. In the present case, the lift curve slope at the Mach number of 0.3 was derived from linear theory. The integration of the state equations was again performed using the Adams-Bashforth ODE solver $\mathcal{D}\mathcal{E}/\mathcal{S}\mathcal{T}\mathcal{E}\mathcal{P}$.

The predictions in Fig. 9 are compared with CFD results based on a TSD code.³³ Such CFD results typically represent close to the state-of-the-art in unsteady aerodynamic modeling, although at a fairly large computational cost. It can be seen that the present predictions for the unsteady lift during the vortex encounter are in excellent agreement with the TSD results. Quasisteady theory (as typically used in some forms of rotor analysis) predicts maximum and minimum lift coefficients several times those shown in Fig. 9, and is not shown here to preserve clarity. On the other hand, unsteady incompressible theory (essentially convolution with the Küssner function²⁹) predicts the same qualitative lift behavior as the TSD solution, but the results in Fig. 9 clearly show a much larger peak-to-peak value of lift. As mentioned previously, this effect is often all too apparent in many helicopter rotor

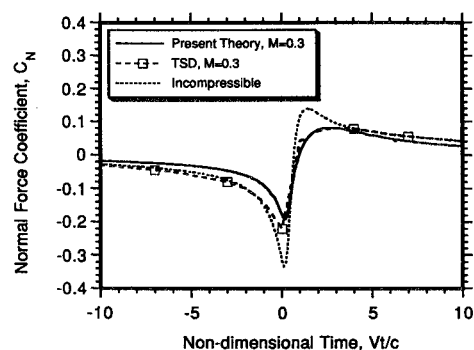


Fig. 9 Prediction of unsteady lift during a vortex encounter.

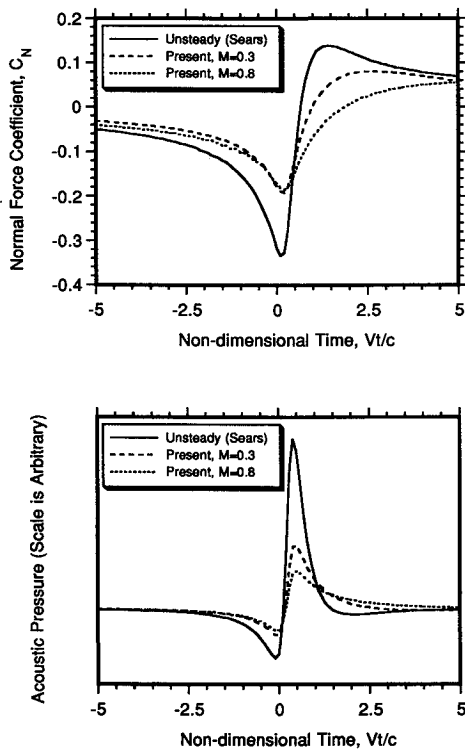


Fig. 10 Prediction of unsteady lift and acoustic during a vortex encounter at various Mach numbers.

analyses that use unsteady aerodynamic modeling, but fail to account for the proper compressibility effects on the unsteady aerodynamics. Of course, a simple quasisteady linearized compressibility scaling to the lift curve slope alone will clearly make these predictions even worse.

Figure 10 shows further results for the unsteady lift and corresponding acoustic pressure obtained during a BVI encounter at the same conditions as those in Fig. 9. The far-field acoustic pressure is related, in the compact source limit, to the time derivative of the unsteady lift on the airfoil. This information is immediately available in the present form of solution since the time derivatives of the aerodynamic states are already computed by the ODE solver. Note that the acoustic pressure in Fig. 10 is unscaled since the distance or path of a reference point in the far field is not specified.

As with the previous case, note the effects of compressibility which essentially produce an attenuation in the peak-to-peak values of the lift. This is despite a higher overall lift curve slope at the higher Mach numbers, which based on incompressible (but unsteady) assumptions might be expected to produce a higher overall peak-to-peak lift. It is significant that when compressibility effects are properly introduced through the form of the indicial (gust) lift function, the opposite effect is obtained, and the peak-to-peak lift during the interaction is reduced. This is mainly because in subsonic compressible flow the unsteady airloads take much longer to readjust to the rapidly changing effective angle of attack induced by the vortex. Similar results of the effects of compressibility for this type of BVI problem are shown in the work of Adamczyk.³⁵

The corresponding acoustic pressure in the lower of Fig. 10 also reaffirms the important effects of compressibility. The most striking difference is that obtained between incompressible unsteady theory and the compressible flow results at the somewhat low Mach number of 0.3. Again, the application of a quasisteady linearized compressibility correction to the incompressible unsteady result (convolution with the Küssner function) will make these predictions even less attractive. In all cases, note that the influence of the vortex affects the acoustic signature only when about two chord lengths upstream and downstream of the airfoil. The transient nature

of the pressure spike obtained is essentially one source of helicopter rotor noise that has become well known as blade slap.

Summary and Conclusions

The primary objective of the present work has been to obtain improved forms of approximate indicial lift functions, generalized in terms of Mach number and pitch axis location, that are in a form suitable for practical calculations of the unsteady lift on airfoils in subsonic flow. It has been shown that when using the known initial and asymptotic behavior of the indicial lift, and by the use of some exact solutions for the indicial response at earlier values of time, it is possible to derive the intermediate behavior of the indicial response from relatively sparse numbers of measurements of the unsteady lift in the frequency domain. The approximation was accomplished in a least-squares sense with the aid of an optimization algorithm. Good correlations with experimental measurements were obtained in the prediction of the corresponding lift transfer function. However, it is clear that the derived indicial lift approximation depends on the quality of the experimental measurements themselves.

To provide further support for the form of the indicial response, a comparison was conducted with a finite-difference result at a Mach number of 0.8 was conducted. Good agreement was found. The general accuracy of the derived indicial response function was also examined by undertaking a time-domain simulation of the unsteady lift on an airfoil during pitch and plunge angle-of-attack forcing. The predictions were compared with experimental measurements of the unsteady lift as a function of angle of attack, with excellent agreement. The significance of compressibility effects on the unsteady lift and acoustic pressure obtained during an airfoil/vortex interaction were also examined. It was shown that the effects of both unsteadiness and compressibility are important in this type of problem, and must be properly included to predict the unsteady aerodynamic response and acoustic pressure.

As a by-product of this research, it is clear that there are somewhat limited published experimental measurements of unsteady lift for airfoils operating under unsteady conditions at the subsonic Mach numbers and reduced frequencies necessary to extract indicial response functions. No one experimental data source was found to be fully adequate, and a number of different data sources were consolidated. There also seems to be a certain amount of scatter in measurements performed on any one airfoil tested in different wind tunnels. The reasons for this are not clear, but may be related to wind-tunnel wall interference effects and this should be carefully considered when using experimental measurements to validate unsteady lift theories.

Acknowledgments

This research was funded by the U.S. Army Research Office under Contract DAAL-03-88-C002. The author wishes to thank the reviewers of this article for their helpful suggestions.

References

- Edwards, J. W., "Unsteady Aerodynamic Modeling and Active Aeroelastic Control," NASA CR-148019, Feb. 1977.
- Dinyavari, M. A. H., and Friedmann, P. P., "Unsteady Aerodynamics in Time and Frequency Domains for Finite Time Arbitrary Motion of Rotary Wings in Hover and Forward Flight," *Proceedings of the AIAA/ASME/ASCE/AHS 25th SDM Conference*, AIAA Paper 84-0988, Palm Springs, CA, May 1984, pp. 266-282.
- Venkatesan, C., and Friedmann, P. P., "A New Approach to Finite-State Modeling of Unsteady Aerodynamics," *Proceedings of the AIAA/ASME/ASCE/AHS 27th SDM Conference*, AIAA Paper 86-0865CP, San Antonio, TX, May 1986, pp. 178-191.
- Beddoes, T. S., "Practical Computation of Unsteady Lift," *Proceedings of the 7th European Rotorcraft Forum*, Aux-en-Provence,

France, Sept. 1982; see also *Vertica*, Vol. 8, No. 1, 1984, pp. 55–71.

⁵Leishman, J. G., and Nugyen, K. Q., "A State-Space Representation of Unsteady Aerodynamic Behavior," *AIAA Journal*, Vol. 28, No. 5, May 1990, pp. 836–845.

⁶Wagner, H., "Über die Entstehung des Dynamischen Auftriebes von Tragflugeln," *Zeitschrift für Angewandte Mathematik und Mechanik*, Bd. 5, Heft 1, Germany, Feb. 1925.

⁷Von Karman, Th., and Sears, W. R., "Airfoil Theory for Non-Uniform Motion," *Journal of the Aeronautical Sciences*, Vol. 5, No. 10, 1938, pp. 379–390.

⁸Sears, W. R., "Operational Methods in the Theory of Airfoils in Nonuniform Motion," *Journal of the Franklin Institute*, Vol. 230, No. 1, 1940, pp. 95–111.

⁹Bisplinghoff, R. L., Ashley, H., and Halfman, R. L., *Aeroelasticity*, Addison-Wesley, Reading, MA, 1955.

¹⁰Peterson, L. D., and Crowley, E. F., "Improved Exponential Time Series Approximation of Unsteady Aerodynamic Operators," *Journal of Aircraft*, Vol. 25, No. 2, 1988, pp. 121–127.

¹¹Eversman, W., and Tewari, A., "Modified Exponential Series Approximation for the Theodorsen Function," *Journal of Aircraft*, Vol. 28, No. 9, 1991, pp. 553–557.

¹²Mazelsky, B., "Numerical Determination of Indicial Lift of a Two-Dimensional Sinking Airfoil at Subsonic Mach Numbers from Oscillatory Lift Coefficients with Calculations for Mach Number of 0.7," NACA TN 2562, Dec. 1951.

¹³Drishler, J. A., "Calculation and Compilation of the Unsteady Lift Functions for a Rigid Wing Subjected to Sinusoidal Gusts and to Sinking Oscillations," NACA TN 3748, Oct. 1956.

¹⁴Dowell, E. H., "A Simple Method for Converting Frequency Domain Aerodynamics to the Time Domain," NASA TM 81844, Aug. 1980.

¹⁵Reissner, E., "On the Application of Mathieu Functions in the Theory of Subsonic Compressible Flow Past Oscillatory Airfoils," NACA TN 2363, May 1951.

¹⁶Mazelsky, B., "On the Noncirculatory Flow About a Two-Dimensional Airfoil at Subsonic Speeds," *Journal of the Aeronautical Sciences*, Vol. 19, No. 12, 1952, pp. 848–849.

¹⁷Leishman, J. G., "Validation of Approximate Indicial Aerodynamic Functions for Two-Dimensional Flow," *Journal of Aircraft*, Vol. 25, No. 10, 1988, pp. 914–922.

¹⁸Lomax, H., "Indicial Aerodynamics," *AGARD Manual of Aeroelasticity*, Pt. II, Nov. 1960, Chap. 6.

¹⁹Lomax, H., Heaslet, M. A., Fuller, F. B., and Sluder, L., "Two and Three Dimensional Unsteady Lift Problems in High Speed Flight," NACA Rept. 1077, 1952.

²⁰Heaslet, M. A., and Spreiter, J. R., "Reciprocity Relations in Aerodynamics," NACA Rept. 1119, Feb. 1953.

²¹Mazelsky, B., and Drischler, J. A., "Numerical Determination of Indicial Lift and Moment Functions of a Two-Dimensional Sinking and Pitching Airfoil at Mach Numbers 0.5 and 0.6," NACA TN 2739, 1952.

²²Mazelsky, B., "Determination of Indicial Lift and Moment of a Two-Dimensional Pitching Airfoil at Subsonic Mach Numbers from Oscillatory Coefficients with Numerical Calculations for a Mach Number of 0.7," NACA TN 2613, Feb. 1952.

²³Tyler, J. C., and Leishman, J. G., "Analysis of Pitch and Plunge Effects on Unsteady Airfoil Behavior," *Proceedings of the 47th Annual Forum of the American Helicopter Society*, Phoenix, AZ, May 6–8, 1991, pp. 69–82.

²⁴Liiva, J., Davenport, F. J., Grey, L., and Walton, I. C., "Two-Dimensional Tests of Airfoils Oscillating Near Stall," USAAVLABS TR 68-13, April 1968.

²⁵Wood, M. E., "Results of Oscillatory Pitch and Ramp Tests on the NACA0012 Blade Section," Aircraft Research Association, Memo. 220, Bedford, England, UK, pp. 1979.

²⁶Davis, S. S., and Malcolm, G. N., "Experimental Unsteady Aerodynamics of Conventional and Supercritical Airfoils," NASA TM 81221, 1980.

²⁷McCroskey, W. J., "The Effects of Gusts on the Fluctuating Airloads of Airfoils in Transonic Flow," *Journal of Aircraft*, Vol. 22, No. 3, 1985, pp. 236–243.

²⁸Shampine, L. F., and Gordon, M. K., *Computer Solution of Ordinary Differential Equations—The Initial Value Problem*, W. H. Freeman and Co., San Francisco, CA, 1975.

²⁹Sears, W. R., "Aerodynamics, Noise and the Sonic Boom," *AIAA Journal*, Vol. 7, No. 4, 1969, pp. 577–586.

³⁰Widnal, S., "Helicopter Noise Due to Blade Vortex Interaction," *Journal of the Acoustical Society of America*, Vol. 50, No. 1, Pt. 2, 1971, pp. 345–365.

³¹Amiet, R. K., "Airfoil Gust Response and the Sound Produced by Airfoil-Vortex Interaction," *Journal of Sound and Vibration*, Vol. 107, No. 3, 1986, pp. 487–506.

³²McCroskey, W. J., and Goojorian, P. M., "Interactions of Airfoils with Gusts and Concentrated Vortices in Unsteady Transonic Flow," AIAA Paper 83-1691, July 1983.

³³Srinivasan, G. R., and McCroskey, W. J., "Numerical Simulations of Unsteady Airfoil Interactions," *Vertica*, Vol. 11, Nos. 1 and 2, 1987, pp. 3–28.

³⁴Yamauchi, G. K., Heffernan, R. M., and Gaubert, M., "Correlation of SA349/2 Helicopter Flight Test Data with a Comprehensive Rotorcraft Model," *Journal of the American Helicopter Society*, Vol. 33, No. 2, 1988, pp. 31–42.

³⁵Adamczyk, J. J., "Passage of a Swept Airfoil Through an Oblique Gust," *Journal of Aircraft*, Vol. 11, No. 5, 1974, pp. 281–287.